Jet Tomography of High-Energy Nucleus-Nucleus Collisions at Next-to-Leading Order

Ivan Vitev[1] and Ben-Wei Zhang[2]

[1]*Theoretical Division, Los Alamos National Laboratory, MS B238, Los Alamos, New Mexico 87545, USA*
[2]*Key Laboratory of Quark Lepton Physics, Hua-Zhong Normal University, Ministry of Education, China*

(Received 26 October 2009; published 29 March 2010)

We demonstrate that jet observables are highly sensitive to the characteristics of the vacuum and the in-medium QCD parton showers and propose techniques that exploit this sensitivity to constrain the mechanism of quark and gluon energy loss in strongly interacting plasmas. As a first example, we calculate the inclusive jet cross section in high-energy nucleus-nucleus collisions to $O(\alpha_s^3)$. Theoretical predictions for the medium-induced jet broadening and the suppression of the jet production rate due to cold and hot nuclear matter effects in Au + Au and Cu + Cu reactions at RHIC are presented.

DOI: 10.1103/PhysRevLett.104.132001 PACS numbers: 13.87.−a, 12.38.Mh, 25.75.−q

Hadronic jets [1], collimated showers of energetic final-state particles, have long been regarded as the main tool to understand hard scattering ($Q^2 \gg \Lambda^2_{\rm QCD}$) processes in $e^+ + e^-$, semi-inclusive deeply inelastic scattering, and hadron-hadron collisions from first-principles in quantum chromodynamics (QCD). Jets are easily accessible by experiment and their landmark discovery has, arguably, stimulated some of the most important developments in the perturbation theory of strong interactions. At present, cross sections for processes involving jets are routinely calculated at next-to-leading-order (NLO) and next-to-next-to-leading-order results are also becoming available [2,3].

An unprecedented possibility exists today to extend the theory of jets to energetic reactions with large nuclei ($A + A$) [4]. Experimental advances at this interface between particle and nuclear physics have already allowed proof-of-principle measurements of jets at the relativistic heavy ion collider (RHIC) [5]. In this Letter, we present the first calculation of jet cross sections and jet substructure for Au + Au and Cu + Cu reactions at RHIC that includes both NLO perturbative effects and effects of the nuclear medium. We demonstrate how jet observables can be used to gain insight into the mechanisms of parton interaction and energy loss [6] in hot, dense, and strongly-interacting quark-gluon plasmas (QGPs) that are created in such reactions. We determine quantitatively the relation between the in-medium modification and broadening of parton showers in the QGP and the suppression in the observed cross section as a function of the jet cone radius R. Owing to their differential nature, jet observables will soon place stringent constraints [5,7] on the approximations and theoretical model assumptions that underlay the current competing approaches to quark and gluon energy loss in hot and dense QCD matter. Such discriminating power cannot be achieved with measurements of leading particle quenching. This will, in turn, help eliminate the uncomfortably large systematic uncertainty in the extraction of the plasma properties, such as its density and transport coefficients [8].

To take full advantage of jet physics in reactions with ultrarelativistic nuclei, calculations at $O(\alpha_s^3)$ are required [9]. In fact, the lowest order QGP-induced parton splitting is also manifested in experimental observables at the same $O(\alpha_s^3)$. With the shortcut notation $d\{E_T, y, \phi\}_n = \prod_{i=1,n} dy_i \prod_{j=2,n} E_{T_j} d\phi_j$ for the independent final-state parton variables in the collinear factorization approach, the simplest inclusive jet cross section at NLO can be expressed as follows [9]:

$$\frac{d\sigma^{\rm jet}}{dE_T dy} = \frac{1}{2!}\int d\{E_T, y, \phi\}_2 \frac{d\sigma[2\to 2]}{d\{E_T, y, \phi\}_2} S_2(\{E_T, y, \phi\}_2) + \frac{1}{3!}\int d\{E_T, y, \phi\}_3 \frac{d\sigma[2\to 3]}{d\{E_T, y, \phi\}_3} S_3(\{E_T, y, \phi\}_3). \tag{1}$$

Here, E_{Ti}, y_i, ϕ_i are the transverse energy, rapidity, and azimuthal angle of the i-th particle ($i = 1, 2, 3$), respectively, and $\sigma[2\to 2]$, $\sigma[2\to 3]$ represent the production cross sections with two and three final-state partons. In Eq. (1) S_2, S_3 are phase space constraints and $S_2 = \sum_{i=1}^2 S(i) = \sum_{i=1}^2 \delta(E_{T_i} - E_T)\delta(y_i - y)$ identifies the jet with its parent parton. Hence, only at NLO can the dependence of the experimental observables on the jet cone radius R and the jet finding algorithms [2,9] be theoretically investigated. For an angular separation $R_{ij} = \sqrt{(y_i - y_j)^2 + (\phi_i - \phi_j)^2}$, defined for any possible parton pair (i, j),

$$S_3 = \sum_{i<j} \delta(E_{T_i} + E_{T_j} - E_T)\delta\left(\frac{E_{T_i} y_i + E_{T_j} y_j}{E_{T_i} + E_{T_j}} - y\right) \times \theta(R_{ij} < R_{\rm rc}) + \sum_i S(i) \prod_{j\neq i} \theta\left(R_{ij} > \frac{(E_{T_i} + E_{T_j})R}{\max(E_{T_i}, E_{T_j})}\right). \tag{2}$$

In Eq. (2), $R_{\rm rc} = \min(R_{\rm sep}R, \frac{E_{T_i}+E_{T_j}}{\max(E_{T_i},E_{T_j})}R)$ determines when two partons should be recombined in a jet. Here,

$1 \leq R_{\rm sep} \leq 2$ is introduced to take into account features of experimental cone algorithms, employed to improve infrared safety. Equation (2) establishes a correspondence between the commonly used jet finders and the perturbative calculations to $O(\alpha_s^3)$ with the goal of providing accurate predictions for comparison to data. For example, $R_{\rm sep} = 2$ yields a midpoint cone algorithm, and $R_{\rm sep} = 1$ corresponds to the k_T algorithm [2,10]. R is the cone size or parton separation parameter, respectively.

In the top panel of Fig. 1, we show a comparison of the NLO calculation [9] of the inclusive jet cross section at $\sqrt{s} = 200$ GeV $p + p$ collisions at RHIC to the STAR experimental measurement which uses a midpoint cone algorithm [11] in the pseudorapidity range $0.2 \leq |\eta| \leq 0.8$. Very good agreement between data and theory is achieved with a standard choice for the renormalization and factorization scales $\mu_R = \mu_f = E_T$. Variation of these scales within $(E_T/2,\ 2E_T)$ leads to less than $(+10\%, -20\%)$ variation of the jet cross section. The bottom panel of Fig. 1 illustrates the significant dependence of $d\sigma^{\rm jet}/dy\,dE_T$ on the cone size R, which, even in $p + p$ reactions, can exceed a factor of 2. Analytically, the $\ln(R/R_0)$ scaling of the cross section can be understood from the $1/r$ angular behavior of the perturbative QCD splitting kernel. Further insight into the underlying parton dynamics can be gained by examining the jet substructure, often characterized by the differential jet shape:

$$\psi(r, R) = \frac{d}{dr}\left\{\frac{\sum_i E_{T_i}\theta(r - R_{i,\rm jet})}{\sum_i E_{T_i}\theta(R - R_{i,\rm jet})}\right\}. \quad (3)$$

In Eq. (3), i stands for the sum over all particles in this jet and $\int_0^R \psi(r, R)dr = 1$. Analytically, jet shapes can be evaluated as follows [4,10]:

$$\psi^{\rm vac.}(r, R) = \psi_{\rm coll}(r, R)[P_{\rm Sudakov}(r, R) - 1] + \psi_{\rm LO}(r, R) + \psi_{i,\rm LO}(r, R) + \psi_{\rm PC}(r, R) + \psi_{i,\rm PC}(r, R). \quad (4)$$

In Eq. (4), the first term represents the contribution from the Sudakov-resummed small-angle parton splitting; the second and third terms give the leading-order final-state and initial-state contributions, respectively; the last two terms come from power corrections $\propto Q_0/E_T$, $Q_0 \simeq$ 2–3 GeV, when one integrates over the Landau pole in the modified leading logarithmic approximation (MLLA). This approach was shown to provide a very good description of the differential intrajet energy flow at the Tevatron [4], as measured by CDF II [12]. Thus, reliable predictions for the jet substructure in $p + p$ reactions at RHIC can be obtained and used as a baseline to study the distortion of jet shapes in more complex systems, such as $p + A$ and $A + A$. An example of $\psi^{\rm vac.}(r, R = 0.4)$ for a quark jet of $E_T = 30$ GeV is shown in Fig. 2.

When compared to a parton shower in the vacuum, the medium-induced quark and gluon splittings have noticeably different angular and lightcone momentum fraction dependencies [4,13]. In particular, for energetic partons propagating in hot and dense QCD matter, the origin of the coherent suppression of their radiative energy loss, known as the Landau-Pomeranchuk-Migdal effect, can be traced to the cancellation of the collinear radiation at $r < m_D/\langle\omega(m_D, \lambda_g, E_T)\rangle$ [13]. Here, the Debye screening scale $m_D = gT\sqrt{1 + N_f/6}$ and $\langle\omega\rangle \simeq$ few GeV. Thus, the medium-induced component of the jet, which is given by the properly normalized gluon bremsstrahlung intensity spectrum $\psi^{\rm med}(r, R) \propto dI^{\rm rad}/d\omega\,dr$ within the cone, has a characteristic large-angle distribution away from the jet axis. This is illustrated in Fig. 2 for central Au + Au and central Cu + Cu collisions at RHIC. We emphasize that accurate numerical simulations, taking into account the geometry of the heavy ion reaction, the longitudinal

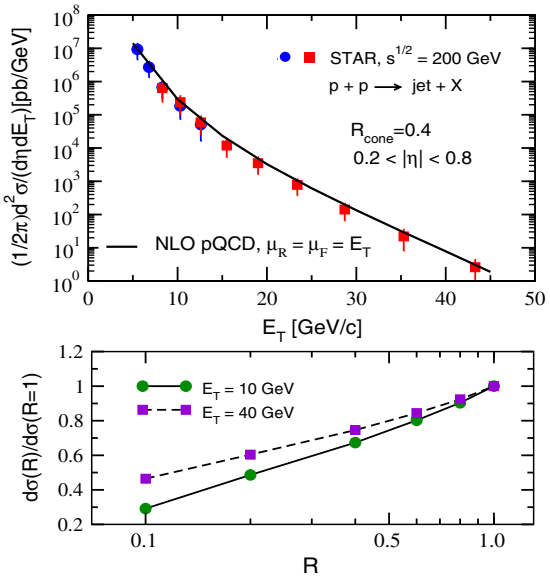

FIG. 1 (color online). Comparison of the NLO calculation to STAR experimental data [11] on the inclusive jet cross section for $R = 0.4$ (top panel). The variation of the jet cross section with the cone size R for $E_T = 10, 40$ GeV around midrapidity at RHIC is also shown (bottom panel).

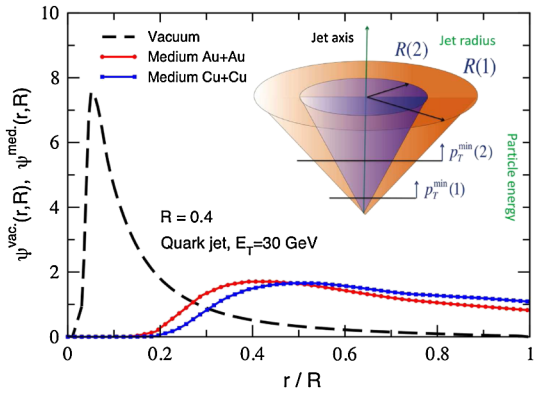

FIG. 2 (color online). The differential jet shape in vacuum $\psi^{\rm vac.}(r, R)$ is contrasted to the medium-induced shape $\psi^{\rm med.}(r, R)$ by a $E_T = 30$ GeV quark in Au + Au and Cu + Cu collisions at $\sqrt{s_{NN}} = 200$ GeV. The insert illustrates a method for studying the characteristics of these parton showers.

Bjorken expansion of the QGP, and the constraints imposed by its experimentally measured entropy density per unit rapidity [4], have been performed for all physics results quoted in this Letter.

One can exploit the differences between the vacuum and the in-medium parton showers by varying the cone radius R ($R_{i,\mathrm{jet}} < R$) and a cut p_T^{min} ($E_{T_i} > p_T^{\mathrm{min}}$) for the particles "$i$" that constitute the jet, to gain sensitivity to the properties of the QGP and to the mechanisms of parton energy loss in hot and dense QCD matter. This is illustrated in the insert of Fig. 2. The most easily accessible experimental feature of jet production in nuclear collisions is, arguably, the suppression of the inclusive cross section in heavy ion reaction compared to the binary collision scaled, $\propto\langle N_{\mathrm{bin}}\rangle$, production rate in elementary nucleon-nucleon reactions [4]:

$$R_{AA}^{\mathrm{jet}}(E_T; R, p_T^{\mathrm{min}}) = \frac{\frac{d\sigma^{AA}(E_T;R,p_T^{\mathrm{min}})}{d^2E_T\,dy}}{\langle N_{\mathrm{bin}}\rangle\frac{d\sigma^{pp}(E_T;R,p_T^{\mathrm{min}})}{d^2E_T\,dy}}. \tag{5}$$

Equation (5) defines a two-dimensional jet attenuation pattern versus R and p_T^{min} for every fixed E_T. In contrast, for the same E_T, inclusive particle quenching is represented by a single value related to the $R \to 0$ and $p_T^{\mathrm{min}} \gg \langle\omega\rangle$ limit in Eq. (5). Thus, jet observables are much more differential and, hence, immensely more powerful than leading particles and leading particle correlations in their ability to discriminate between the competing physics mechanisms of quark and gluon energy loss in dense QCD matter and between theoretical model approximations to parton dynamics in the QGP.

We now focus on the first complete theoretical result at NLO for R_{AA}^{jet} versus the jet cone size R for Au + Au and Cu + Cu collisions at RHIC. We use the reaction operator approach to non-Abelian energy loss [14], in the limit of weak coupling between the jet and the plasma with $\alpha_s \sim 0.3$, to evaluate the probability distribution $P_{q,g}(\epsilon, E)$ that quarks and gluons, respectively, will lose a fraction of their energy $\epsilon = \sum_i \omega_i/E$ due to medium-induced bremsstrahlung. Next, we determine the fraction of this energy that will be redistributed inside the jet:

$$f_{q,g} \equiv f(R, p_T^{\mathrm{min}})_{q,g} = \frac{\int_0^R dr \int_{p_T^{\mathrm{min}}}^{E_T} d\omega \frac{dI_{q,g}^{\mathrm{rad}}}{d\omega\,dr}}{\int_0^{R^\infty} dr \int_0^{E_T} d\omega \frac{dI_{q,g}^{\mathrm{rad}}}{d\omega\,dr}}. \tag{6}$$

While such redistribution may affect the jet shape, it will not affect the jet cross section. For example, when $R \to R^\infty$ and $p_T^{\mathrm{min}} \to 0$ ($f_{q,g} = 1$) final-state QGP-induced effects to inclusive or tagged jet cross sections vanish. Parton interactions in the strongly interacting plasma, however, are not the only many-body QCD effects that will alter the measured jet cross section. Cold nuclear matter (CNM) effects prior to the QGP formation [15] must also be included in accurate theoretical calculations of hard probes production in nuclear collisions, and we first evaluate $\frac{d\sigma^{\mathrm{CNM,NLO}}}{d^2E_T\,dy}$. We find that in the kinematic region of interest, 10 GeV $\leq E_T \leq$ 50 GeV around midrapidity at RHIC $\sqrt{s_{NN}} =$ 200 GeV collisions, the EMC effect and initial-state energy loss [15] play a dominant role. Next, we determine the relative fractions $n_{q,g}$ of quark and gluon jets in this inclusive cross section ($n_q + n_g = 1$). These are well defined at leading order [16] and separation of the inclusive cross section into $\frac{d\sigma_{q,g}^{\mathrm{CNM,NLO}}}{d^2E_T\,dy}$ is necessary to properly describe parton energy loss in the QGP, which scales with the quadratic Casimir in the corresponding representation of SU(3) ($C_A/C_F = 2.25$). At NLO, there exists an ambiguity of $O(\alpha_s)$ in this separation [16], which has a very small effect on inclusive jet observables.

We calculate the medium-modified jet cross section per binary nucleon-nucleon scattering as follows ($p_T^{\mathrm{min}} = 0$):

$$\frac{1}{\langle N_{\mathrm{bin}}\rangle}\frac{d\sigma^{AA}(R)}{d^2E_T\,dy} = \int_{\epsilon=0}^1 d\epsilon \sum_{q,g} P_{q,g}(\epsilon, E)\frac{1}{[1-(1-f_{q,g})\epsilon]^2} \times \frac{d\sigma_{q,g}^{\mathrm{CNM,NLO}}(R)}{d^2E_T'\,dy}. \tag{7}$$

In Eq. (7), $(1 - f_{q,g})\epsilon$ represents the fraction of the energy of the parent parton that the medium redistributes outside of the cone of radius R. The measured cross section is then a probabilistic superposition of the cross sections of protojets of initially larger energy $E_T' = E_T/[1 - (1 - f_{q,g}) \cdot \epsilon]$. Our results for the nuclear modification factor of inclusive jets R_{AA}^{jet} in central Au + Au and Cu + Cu collisions with $\sqrt{s_{NN}} = 200$ GeV at RHIC are presented in Fig. 3. Each band illustrates a calculation for a ~20% increase in the rate of parton energy loss (lower bound) relative to our default simulation (upper bound). Experimental data on leading π^0 suppression for these reactions is only included for reference. A continuous variation of R_{AA}^{jet} with the cone radius R is clearly observed in Fig. 3 and shows the sensitivity of the inclusive jet cross section in high-energy nuclear collisions to the characteristics of QGP-induced parton shower. For $R \leq 0.2$, the quenching of jets approximates the already observed suppression in the production rate of inclusive high-p_T particles. It should be noted that in our theoretical calculation, CNM effects contribute close to 1/2 of the observed attenuation for $E_T \geq 30$ GeV. These can be drastically reduced at all E_T by taking the ratio of two differential cross section measurements for different cone radii R_1 and R_2. A few selected examples are shown in the inserts of Fig. 3.

Inclusive jet cross sections and jet shapes in nuclear collisions are closely related [4]:

$$\psi_{\mathrm{tot.}}\left(\frac{r}{R}\right) = \int_{\epsilon=0}^1 d\epsilon \sum_{q,g} \frac{P_{q,g}(\epsilon,E)\chi_{q,g}(R;E_T,E_T')}{[1-(1-f_{q,g})\cdot\epsilon]^3} \times \left[(1-\epsilon)\psi_{\mathrm{vac.}}^{q,g}\left(\frac{r}{R};E'\right) + f_{q,g}\epsilon\psi_{\mathrm{med.}}^{q,g}\left(\frac{r}{R};E'\right)\right], \tag{8}$$

$\chi_{q,g}(R; E_T, E_T')/\langle N_{\mathrm{bin}}\rangle = \frac{d\sigma_{q,g}^{\mathrm{CNM,NLO}}(R,E_T')}{d^2E_T'\,dy} / \frac{d\sigma^{AA}(R)}{d^2E_T\,dy}$. It should

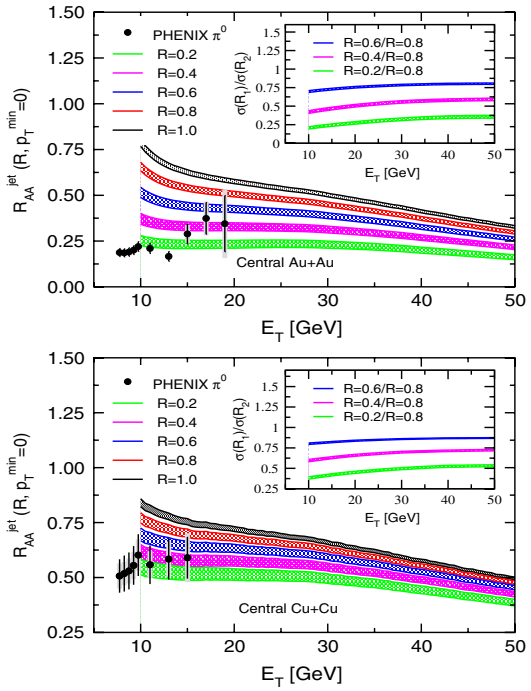

FIG. 3 (color online). Transverse energy dependent nuclear modification factor $R_{AA}^{\rm jet}$ for different cone radii R in $b = 3$ fm Au + Au (top panel) and Cu + Cu (bottom panel) collisions at $\sqrt{s_{NN}} = 200$ GeV. Inserts show ratios of jet cross sections for different R in nuclear reactions versus E_T.

be noted that vacuum and medium-induced parton showers become more collimated with increasing E_T', and the mean relative jet width $\langle r/R\rangle = \int_0^1 d(r/R)(r/R)\psi(r/R)$ is reduced [4]. Consequently, the striking suppression pattern for jets, shown in Fig. 3, can be accompanied by a very modest growth in the observed $\langle r/R\rangle_{\rm tot.}$. We show in Table I the relative widths in the vacuum, for a hypothetical case of complete parton energy loss ($P_{q,g}(\epsilon) = \delta(1-\epsilon)$) that falls inside of R ($f_{q,g} = 1$), and for our realistic simulation of $E_T = 30$ GeV jets of $R = 0.4$ in central Au + Au and Cu + Cu collisions at RHIC. We find that, on average, jet broadening $\Delta\langle r/R\rangle = (\langle r/R\rangle_{\rm tot.} - \langle r/R\rangle_{\rm vac.})/\langle r/R\rangle_{\rm vac.}$ is $<5\%$. Larger effects are expected near the core $r \to 0$ and the periphery $r \to R$ of the jet [4].

In summary, the principle goal of this Letter is to bring into focus the immense possibilities that jets offer as tomographic probes of the QGP created in ultrarelativistic nuclear collisions. To demonstrate the unprecedented sensitivity of jet observables to the characteristics of the vacuum and the medium-induced parton showers, we presented first results for the related cross sections and shapes as a function of the cone radius R at next-to-leading-order $O(\alpha_s^3)$ in $p + p$, central Au + Au, and central Cu + Cu collisions at RHIC. Our theoretical predictions include a most detailed account of cold and hot nuclear matter effects on jet production and distortion in heavy ion reactions and are of immediate relevance to upcoming

TABLE I. Mean relative jet radii $\langle r/R\rangle$ in the vacuum, for complete parton energy loss in the medium, and for the realistic case of jets in Au + Au and Cu + Cu collisions at RHIC. We considered a radius $R = 0.4$ and transverse energy $E_T = 30$ GeV at $\sqrt{s_{NN}} = 200$ GeV. The fractional QGP-induced broadening $\Delta\langle r/R\rangle$ is also shown.

$\langle r/R\rangle$	Vacuum	Medium	Total	Δ
Au + Au	0.271	0.601	0.283	4%
Cu + Cu	0.271	0.640	0.272	0.4%

PHENIX and STAR experimental measurements. We fully expect that this work will inspire future studies of inclusive and tagged jets, jet substructure, and event shape observables. In their entirety, such studies will provide first-principles insights into the many-body QCD parton dynamics at ultrarelativistic energies and shed light on the relative importance of collisional versus radiative energy loss and on the applicability of weak versus strong jet-medium coupling regimes.

We thank D. E. Soper and F. I. Olness for helpful discussions.

[1] G. Sterman and S. Weinberg, Phys. Rev. Lett. **39**, 1436 (1977); R. P. Feynman, R. D. Field, and G. C. Fox, Phys. Rev. D **18**, 3320 (1978).
[2] J. M. Campbell, J. W. Huston, and W. J. Stirling, Rep. Prog. Phys. **70**, 89 (2007); S. D. Ellis *et al.*, Prog. Part. Nucl. Phys. **60**, 484 (2008).
[3] F. I. Olness and D. E. Soper, arXiv:0907.5052.
[4] I. Vitev, S. Wicks, and B. W. Zhang, J. High Energy Phys. 11 (2008) 093; I. Vitev, B. W. Zhang, and S. Wicks, Eur. Phys. J. C **62**, 139 (2009).
[5] S. Salur, Nucl. Phys. **A830**, 139C (2009); M. Ploskon, Nucl. Phys. **A830**, 255C (2009).
[6] X. N. Wang and M. Gyulassy, Phys. Rev. Lett. **68**, 1480 (1992).
[7] N. Grau, Nucl. Phys. **A830**, 797C (2009); D. d'Enterria *et al.*, J. Phys. G **34**, 2307 (2007).
[8] S. A. Bass *et al.*, Phys. Rev. C **79**, 024901 (2009).
[9] S. D. Ellis, Z. Kunszt, and D. E. Soper, Phys. Rev. Lett. **64**, 2121 (1990); Z. Kunszt and D. E. Soper, Phys. Rev. D **46**, 192 (1992).
[10] M. H. Seymour, Nucl. Phys. **B513**, 269 (1998).
[11] B. I. Abelev *et al.* (STAR Collaboration), Phys. Rev. Lett. **97**, 252001 (2006).
[12] D. E. Acosta *et al.* (CDF Collaboration), Phys. Rev. D **71**, 112002 (2005).
[13] I. Vitev, Phys. Lett. B **630**, 78 (2005).
[14] M. Gyulassy, P. Levai, and I. Vitev, Phys. Rev. Lett. **85**, 5535 (2000); I. Vitev, Phys. Rev. C **75**, 064906 (2007).
[15] I. Vitev and B. W. Zhang, Phys. Lett. B **669**, 337 (2008); R. Sharma, I. Vitev, and B. Zhang, Phys. Rev. C **80**, 054902 (2009).
[16] M. Dasgupta, L. Magnea, and G. Salam, J. High Energy Phys. 02 (2008) 055.